

# System Modeling and Robust Design of Microaccelerometer Using Piezoelectric Thin Film

Jyh-Cheng YU<sup>1</sup>, Ching-Bin LAN<sup>2</sup>

Department of Mechanical Engineering  
National Taiwan University of Science and Technology  
Taipei, Taiwan 106, R.O.C.

jcyu@mail.ntust.edu.tw<sup>1</sup>, lan@bison.me.ntust.edu.tw<sup>2</sup>

## Abstract

*This paper starts from the structure analysis and system modeling of piezoelectric microaccelerometer using piezoelectric thin film. The simulation model demonstrates the interaction of structure variables, piezoelectric material parameters, and amplification circuit design to the sensor performance. However, manufacturing error results in the variations of design variables, which has significant effects on sensor accuracy. The proposed system model is applied to the parameter design of microaccelerometer. The paper conducts the design optimization and robustness analysis using Taguchi's method to reduce the sensitivity of the sensor response to the dimensional errors and variations of material properties. A FEM study is applied to verify the theoretical model and design improvement.*

*Keywords*—Sensor design, PZT, Robust Design, Taguchi.

## 1. Introduction

The research of Micro-ElectroMechanical-System (MEMS) has drawn lots of attention in the recent years due to the urge of miniaturization of consuming products. The advance of micro-machining process has made possible the production of a three-dimensional microstructure on a silicon wafer. Successful examples include cantilever beam, bridge, diaphragm, gear, and micromotor. Microsensors consist of microstructures, piezoelectric transducer, and charge amplifier, which can be easily integrated in a single chip using existed manufacturing process of integrated circuit. Compared with conventional bulk sensors, microsensors have many advantages such as miniature configuration, lower cost, better response characteristics, and better controllability.

Because of its advantages of high electro-mechanical coupling factor, high electric impedance, and temperature stability, PZT ( $\text{PbZr}_x\text{Ti}_{1-x}\text{O}_3$ ) transducers

are very promising in sensor and actuator [1]. The quality of piezoelectric thin films used to be a constraint in the application of micro-transducers. However, the continuous breakthrough of the coating process of ceramic thin film has greatly improved the film quality, which raises lots of interests in the relevant research [2].

Most literatures focus on the manufacturing aspects of microsensors [3-5]. Some literatures [6,7] conduct FEM analysis of the thin film on a flexible structure subject to bending moment, torsion, and transverse shear to study the influence of structure stresses on the static and dynamic piezoelectric properties. Gianchandani and Grary [8] provide a parametric modeling of a microaccelerometer using response-surface method to identify the optimal location of suspension beams. van Kampen and Wolffenbuttel [9] conduct an extensive modeling of seismic microstructure to illustrate the mechanical behavior of bulk-micromachined silicon accelerometers. Nemirovsky et al. [10] design and analyze a piezoelectric thin-film accelerometer of compression type. However, studies on the parameter design of sensor systems are much limited. On the other hand, manufacturing errors from material and process variations will significantly affect the accuracy of sensors. This paper aims to establish the system model of the microaccelerometers using piezoelectric thin film, and applies Taguchi's method to the parameter design of the microstructure to reduce the sensitivity of manufacturing variations to sensor response.

## 2. Typical Model of Accelerometer

Figure 1 represents the general configuration of a seismic-displacement pickup for unidirectional translative motions. The system consists of a mass-spring-damper structure and a displacement transducer. The acceleration  $\ddot{x}_i$  of the moving object is the physical quantity pending investigation.

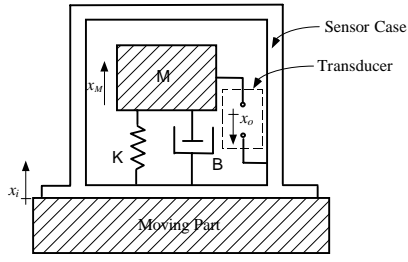


Figure 1. Typical system model of an accelerometer

According to Newton's second law, the governing equation of the seismic mass  $M$  at small displacement is as follows:

$$M\ddot{x}_i = M\ddot{x}_o + B\dot{x}_o + Kx_o \quad (1)$$

The acceleration  $\ddot{x}_i$  of the moving object will cause a relative displacement  $x_o$  of the seismic mass and the sensor base. A piezoelectric transducer is applied to convert the displacement into an electronic signal. The complete system model  $T$  is a combination of a mechanical transfer function  $G_m$  and an electronic transfer function  $G_e$ .

### 2.1 Mechanical Transfer Function

Mechanical transfer function  $G_m$  models the frequency response of the relative displacement  $x_o$  of the seismic mass and the sensor base due to the acting acceleration  $\ddot{x}_i$ . Assume the initial conditions:  $x_o(0) = 0$  and  $\dot{x}_o(0) = 0$ , manipulation of Eq. (1) gives the mechanical transfer function:

$$\frac{x_o}{\ddot{x}_i}(D) = S_m \cdot \frac{w_n^2}{D^2 + 2\zeta w_n D + w_n^2} \quad (2)$$

where  $w_n = \sqrt{\frac{K}{M}}$  is the resonance frequency of structure

$$\zeta = \frac{B}{2\sqrt{KM}} \text{ is the damping ratio}$$

$$S_m \equiv \frac{M}{K} \text{ is the mechanical sensitivity}$$

### 2.2 Electronic Transfer Function

Electronic transfer function  $G_e$  models the frequency response of the relative displacement  $x_o$  and the output voltage  $e_o$  of the displacement transducer. The piezoelectric transducer assumes linear relation between the output charge and the relative displacement  $x_o$  of the seismic mass and the sensor base.

$$Q = K_q \cdot x_o \quad (3)$$

where  $K_q$  is the charge output of unit displacement

The analogous circuit of the piezoelectric transducer system can be simplified to the equivalent model in

Figure 2 [11, pp.261]. Both the transducer and the amplifier have high impedance to prevent the leakage of electric charge. The resulting resistance and the capacitance of the equivalent model are shown in Eqs.(4) and (5).

$$R \equiv \frac{R_{ampl} R_{leak}}{R_{ampl} + R_{leak}} \quad (4)$$

$$C \equiv C_{PZT} + C_{cable} + C_{ampl} \quad (5)$$

where  $R_{leak}$ : PZT leakage resistance  
 $C_{PZT}$ : PZT leakage capacitance  
 $C_{Cable}$ : Cable capacitance  
 $C_{ampl}$ : Amplifier capacitance  
 $R_{ampl}$ : Amplifier resistance

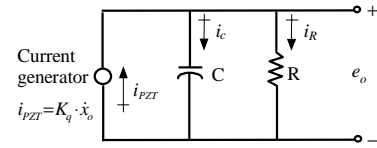


Figure 2. Equivalent circuit model of the piezoelectric transducer system

Analysis of the equivalent circuit will yield the electronic transfer function of the piezoelectric transducer system as follows:

$$\frac{e_o}{x_o}(D) = S_e \cdot \frac{\tau D}{\tau D + 1} \quad (6)$$

where  $S_e \equiv \frac{K_q}{C}$  is the electronic sensitivity

$\tau \equiv RC$  is the time constant of the electric subsystem

### 2.3 System Model of Piezoelectric Accelerometer

The complete system model combines the mechanical and electronic transfer functions as follows:

$$\frac{e_o}{\ddot{x}_i}(D) = S \cdot \frac{\tau D}{\tau D + 1} \cdot \frac{w_n^2}{D^2 + 2\zeta w_n D + w_n^2} \quad (7)$$

where  $S \equiv S_e \cdot S_m = \frac{K_q}{C} \cdot \frac{M}{K}$  is the sensitivity of sensor

Typical frequency range of the accelerometer using  $\pm 5\%$  as accuracy requirement is between  $3/\tau$  and  $w_n/5$  (Figure 3). The low-frequency response is limited by the time constant  $\tau$  of piezoelectric transducer while the high-frequency range is limited by mechanical resonance  $w_n$ . On the other hand, the piezoelectric characteristic  $K_q/C$  and the structure characteristic  $1/w_n^2$  determine the accelerometer sensitivity. Therefore, tradeoffs exist between high frequency response and sensitivity.

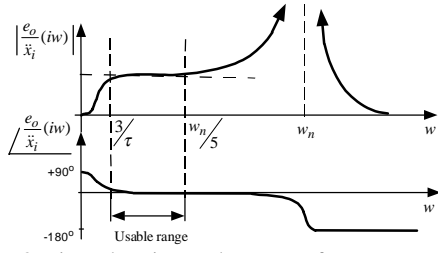


Figure 3. Piezoelectric accelerometer frequency response

### 3. System Modeling of Piezoelectric Micro-accelerometer

#### 3.1 Static Behavior of Microstructure

This paper assumes that the structure of the microaccelerometer consists of a centered seismic mass suspended by four symmetric cantilever beams as shown in Figure 4. When acceleration is acting on the structure, the seismic mass translates up and down with negligible motions in other directions. The piezoelectric transducer consists of an upper electrode, a PZT thin film, and a lower electrode, and is mounted near the fixed end of beam suspension. The transducer assumes the same width  $b$  as the cantilever beam and the length of PZT film  $l_p$  to be half the beam length  $l$  to maximize transducer sensitivity (Figure 5).

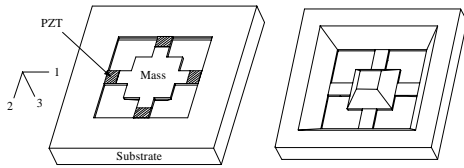


Figure 4. Structure configuration of the microaccelerometer

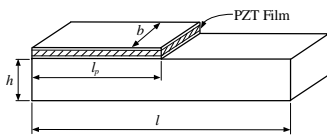


Figure 5. Details of the beam suspension

The mechanical model of the microaccelerometer is based on the following assumptions:

- (1) The weight of the supporting beams is negligible compared with the seismic mass.
- (2) The seismic mass and the rim of structure are rigid.
- (3) The deflections of supporting beams observe linear elasticity and Hooke's Law.
- (4) The seismic mass only translates in the direction-3.
- (5) The PZT film and electrodes are much thinner than supporting beams, and have negligible effect to the beam stiffness.

When the seismic mass is subject to normal acceleration, the inertial force results in a deflection of beam suspension. Because four symmetric beams suspend the seismic mass, the free-body diagram of the suspension beam looks like Figure 6.

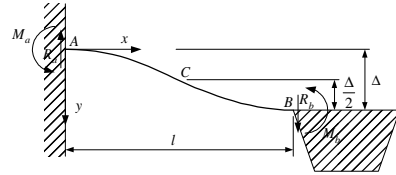


Figure 6. Free-body diagram of suspension beam

If the deflection is small, the differential equation of the deflection of beam is approximated according to Hooke's law as follows.

$$\frac{d^2 y}{dx^2} = -\frac{M}{EI}$$

Assume the bonding between PZT film and beam suspension is perfect. When the inertial force of seismic mass is acting on the beam, the stresses of PZT film in the direction-1 are approximately equal to the stresses on the mounting surface of the beam. Solving the differential equation will yield.

$$T_1 = \frac{M x y}{I} \approx \frac{E h \Delta}{l^2} \left( 3 - \frac{6x}{l} \right) \quad (8)$$

Since the seismic mass is supported by four beams, the total reaction force is  $F=4R_q$ . The stiffness  $K$  of the beam suspension is

$$K = \frac{48EI}{l^3} \quad (9)$$

where  $I$  is the moment of inertia of the rectangular beam

#### 3.2 Seismic Mass

When using bulk-micromachining techniques, the seismic mass is shaped like a truncated pyramid, as shown in Figure 7, due to the anisotropic etching of silicon in KOH.

Simple integration of the structure will give the mass  $M$ .

$$M = \rho \cdot V = \frac{\sqrt{2} \cdot \rho}{6} \left[ l_{Mt}^3 - (l_{Mt} - \sqrt{2} \cdot h_M)^3 \right] + \rho \cdot l_{Mt}^2 \cdot h \quad (10)$$

where  $\rho$  is the density of the material

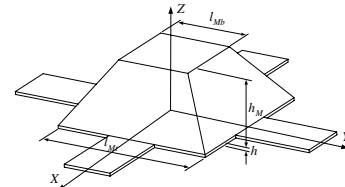


Figure 7. Details of the pyramid shaped seismic mass

### 3.3 System Transfer Function

The system transfer function of piezoelectric microaccelerometer is similar to Eq. (2) with the sensitivity  $S_m$  as follows:

$$S_m \equiv \frac{M}{K} = \frac{Ml^3}{48EI} = \frac{Ml^3}{4Ebh^3} \quad (11)$$

If the PZT is subject to stresses in the direction-1, and the stresses in other directions are all negligible, the electric potential output  $D_3$  between electrodes is as follows for no external electric field.

$$D_3 = d_{31}T_1 \quad (12)$$

Combining Eqs.(8) and (12) the charge output of PZT film is:

$$Q = \int_0^{l_p} D_3 b \, dx = \frac{3d_{31}bEh\Delta l_p}{l^2} \left(1 - \frac{l_p}{l}\right) \quad (13)$$

If the PZT transducers of four supporting beams are connected in series, the total charge output due to unit displacement of seismic mass will be fourfold. Analogous to Eq.(3), the output charge of the PZT transducer due to unit displacement of seismic mass is

$$K_q = \frac{12d_{31}bEhl_p}{l^2} \left(1 - \frac{l_p}{l}\right) \quad (14)$$

Substitution of Eqs.(11) to Eq.(7) yields the system transfer function of the piezoelectric microaccelerometer.

$$\frac{e_o(D)}{\ddot{x}_i} = \frac{3Md_{31}ll_p \left(1 - \frac{l_p}{l}\right)}{h^2C} \cdot \frac{\tau D}{\tau D + 1} \cdot \frac{w_n^2}{D^2 + 2\zeta w_n D + w_n^2} \quad (15)$$

The system model shows that the sensitivity  $S$  of the accelerometer is related to dimensions of beam suspension, piezoelectricity constant  $d_{31}$  of PZT film, seismic mass, and the equivalent capacitance of transducer circuit. The parameter design of piezoelectric microaccelerometer depends on the features of performance desired for particular applications.

### 4. Robust Design of Piezoelectric Microaccelerometer

Design optimization seeks to maximize sensor sensitivity and frequency bandwidth. However, MEMS devices have large relative variations in dimensions and material parameters, which result in response variations. Performance robustness is another importance issue in the parameter design of accelerometers to reduce the sensitivity of sensor accuracy to manufacturing variations.

Robust design reduces the performance deviation by reducing the sensitivity of the design to variations rather than controlling the sources. Taguchi's method [12] is an effective tool of robust design. The method features signal-to-noise ratio, orthogonal array experiments, and analysis of variance to perform a two-step robust optimization.

### 4.1 Robust Design Using Taguchi's Method

The accuracy and reproducibility of microsensors are related to the etching dimensions of microstructure and the uniformity of material characteristic. Dimensional variations of mechanical structure are due to errors of lithographic and micromachining processes [13]. Variations of material characteristics are due to uncontrollable factors in the growing process of piezoelectric film.

Minimization of the response sensitivity to manufacturing variations is essential in the parameter design of microsensors. Figure 8 shows the target configuration of the mechanical structure of microaccelerometer. The mechanical properties of PZT film and silicon substrate are anisotropic. Due to the characteristic of the configuration, the assumption of isotropic properties only lead to negligible error. Table 1 lists the mechanical properties of sensor materials.

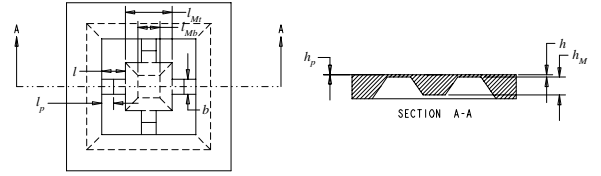


Figure 8. Configuration of micro structure of microaccelerometer

This paper also assumes the characteristic of the amplification circuit as follows: equivalent capacitance  $C=10\text{pF}$  and equivalent resistance  $R=10^{10}\Omega$ . The control factors of the initial design are listed in Table 2. The thickness of PZT film  $h_p$  and the thickness of electrode  $h_e$  are presumed as follows.

$$h_p = 0.3\mu\text{m}$$

$$h_e = 0.2\mu\text{m}$$

Table 1. Material properties in the analysis

	material	Young's modulus (N/m <sup>2</sup> )	Density (kg/m <sup>3</sup> )	Poisson's ratio
Mechanical microstructure	silicon	$1.69 \times 10^{11}$	2330	0.0625
Piezoelectric film	PZT (52/48)	$72.5 \times 10^9$	7550	0.3
Electrodes	platinum	$171 \times 10^9$	21450	0.39

Table 2. Dimensions of the initial design of piezoelectric accelerometer

Length of beam suspension	$l$	400 $\mu\text{m}$
Width of beam suspension	$b$	200 $\mu\text{m}$
Thickness of beam suspension	$h$	15 $\mu\text{m}$
Length of seismic mass	$l_M$	800 $\mu\text{m}$
Thickness of seismic mass	$h_M$	300 $\mu\text{m}$

The output charge of ideal accelerometer assumes a linear relation with acting acceleration in the frequency bandwidth. In another word, the sensitivity of sensor

is fixed at target value. However, actual sensor sensitivity varies due to manufacturing errors and environmental disturbances. Robust design aims to minimize the sensitivity of sensor performance to noise factors.

For illustration simplicity, the noise factors considered in this paper include dimensional errors of microstructure,  $b$ ,  $h$ ,  $l$ ,  $l_M$ ,  $h_M$ , variation of Young's modulus  $E$  of beam suspension, and frequency  $w$  of acting acceleration.

It is a dynamic problem of robust design. However, this study uses the system modeling function to simulate the response of accelerometer, the relation between output signal and acting acceleration is defined by Eq.(15). The sensor design can be simplified as a nominal-the-best problem. The objective function is defined as follows:

$$S/N = 10 \log_{10} \frac{\mu^2}{\sigma^2} \quad (16)$$

where  $\mu$  is the mean and  $\sigma^2$  is the variance of sensor gain of outer array simulations.

We select 3-level factorial design for the control factors and set the initial design as the central level. The frequency of acting acceleration is selected as 4-level, and the rest of noise factors are set as 2-level. The experimental design selects  $L_{18}(2^1 \times 3^7)$  orthogonal array for the control factors, as shown in Table 3, and applies the column merging method to modify  $L_{16}$  orthogonal array to accommodate a 4-level and six 2-level noise factors ( Table 4).

Table 3. Experimental design of inner orthogonal array

	$l$	$b$	$h$	$l_M$	$h_M$	Mean	S/N
1	300	180	10	700	250	1.1434	15.5038
2	300	220	15	800	300	0.7719	19.1410
3	300	220	20	900	350	0.6313	21.5853
4	400	180	10	800	300	3.2188	14.0685
5	400	220	15	900	350	1.9936	18.5755
6	400	220	20	700	250	0.5266	21.6968
7	500	180	15	700	350	1.5987	18.5210
8	500	220	20	800	250	1.1545	21.3503
9	500	220	10	900	300	7.4810	10.7328
10	300	180	20	900	300	0.5961	21.5888
11	300	220	10	700	350	1.2603	15.4802
12	300	220	15	800	250	0.7157	19.1983
13	400	180	15	900	250	1.7218	18.6565
14	400	220	20	700	300	0.5586	21.6415
15	400	220	10	800	350	3.3485	14.3853
16	500	180	20	800	350	1.3052	21.1525
17	500	220	10	900	250	6.8572	10.6950
18	500	220	15	700	300	1.5362	18.7450

Unit:  $\mu\text{m}$

Each design in the inner array is simulated 16 times using the outer orthogonal array. Eq.(15) is used to obtain the sensor gain of each simulation. Mean and signal-to-noise ratio of each design are evaluated as listed in Table 3. Figure 9 and Figure 10 show the effect plots of output means and S/N ratios.

We use the output mean (1.385 mV/m/sec<sup>2</sup>) of the initial design to be the target gain to illustrate the improvement of output deviation of robust design. The effect plots show that factor  $l$  and factor  $l_M$  could

be that scaling factors that have significant effect to mean but little effect to S/N ratio. Taguchi's method adopts a two-step optimization that first set major control factors to the levels maximizing S/N ratio and adjust the output mean to target using scaling factors. The parameters of the robust design of piezoelectric accelerometer are shown in Table 5.

Table 4. Levels of Noise Factorial

	Level 1	Level 2	Level 3	Level 4
$w$	31.416	10493	20954	31416
$\Delta l$	-1.0	+1.0		
$\Delta b$	-1.0	+1.0		
$\Delta h$	-0.8	+0.8		
$\Delta l_M$	-1.0	+1.0		
$\Delta h_M$	-0.3	+0.3		
$\Delta E$	-2.0	+2.0		

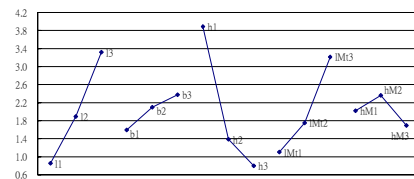


Figure 9. Effect plot of means

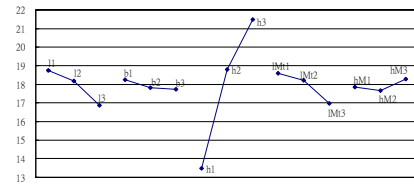


Figure 10. Effect plot of S/N ratio

Table 5. Parameters of the robust design of microstructure

Factor	Size
$l$	442 $\mu\text{m}$
$b$	180 $\mu\text{m}$
$h$	20 $\mu\text{m}$
$l_M$	900 $\mu\text{m}$
$h_M$	350 $\mu\text{m}$

In the modeling of the structure stiffness, this paper assumes the stiffness of electrodes and PZT film is negligible. For verification purpose, we conduct a finite element analysis using ANSYS 5.3 to compare the resonance frequency of the microstructure. Table 6 shows that the resonance frequencies of modeling result and FEM analysis are very close, which demonstrates our assumption is reasonable.

Table 6. Verification of the resonance frequency of microstructure

$F_n$	Modeling result	FEM analysis	Error (%)
Initial Design	25654 Hz	25742 Hz	0.342
Robust Design	26665 Hz	26275 Hz	1.463

We apply the additive model to estimate the S/N ratios of initial and robust designs.

$$S/N_{\text{initial}}(l_2 b_2 h_2 l_{M2} h_{M2}) = m + l_2 + b_2 + h_2 + l_{M2} + h_{M2} = 18.94$$

$$S/N_{\text{opt.}}(l_2 b_1 h_3 l_{M3} h_{M3}) = m + l_2 + b_1 + h_3 + l_{M3} + h_{M3} = 21.46$$

Table 7 lists the S/N ratios of initial and robust designs. The comparison shows that the result from the additive model fairly agrees with the verification experiments, which demonstrates the rationality of the experimental design.

Table 7. S/N ratios of initial and robust designs

S/N	Estimate	Verification
Initial	18.94	18.86
Robust	21.46	21.17
Improvement	2.52	2.31

The robust design has an improvement of 2.31dB in the S/N ratio, which represents a reduction of the variation of sensor sensitivity by 23.4% compared with the initial design. Figure 11 and Figure 12 show the frequency responses of the initial and robust designs. The extent between arrowheads represents the variation of sensor sensitivity due to manufacturing errors. The robust design reduces the sensitivity of performance to noise factors using parameter design, which improves the sensor accuracy without tightening the tolerances of parameters.

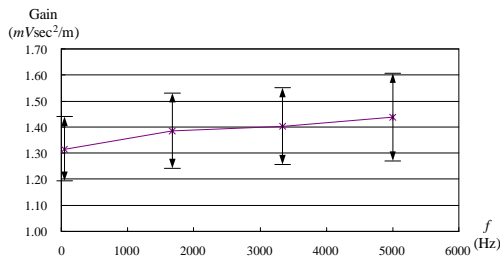


Figure 11. Frequency response and sensitivity variation of initial design

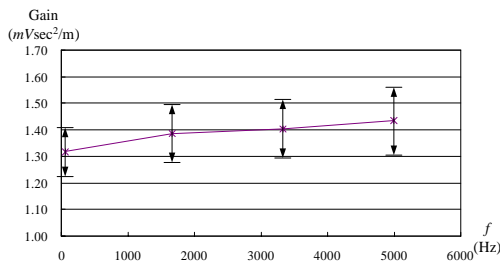


Figure 12. Frequency response and sensitivity variation of robust design

## 5. Conclusion

This paper addresses the system modeling of piezoelectric microaccelerometer. A configuration of multiple-supported structure is used as an example to

derive the design variables. FEM analysis of the resonance frequency of the microstructure shows that errors incurred by the simplifying model are typically negligible. We further illustrate the manufacturing variations that significantly affect the sensor accuracy and frequency bandwidth. Parameter design using Taguchi's method provides a robust design of accelerometer. The robust design reduces the variation of sensor sensitivity by 23.4% compared with the initial design. This study illustrates the procedure and feasibility of design for robustness. Continuous improvement can be achieved by recursive design optimization.

## 6. Acknowledgement

This research is funded by the National Science Council of the ROC under grant NSC 88-2216-E-011-013.

## 7. References

- [1] Polla D. L., and Francis L. F. (1996), "Ferroelectric Thin Films in Microelectromechanical Systems Applications", *MRS Bulletin*, pp. 59-65.
- [2] Okuyama M. (1998) "Microsensors and Microactuators Using Ferroelectric Thin Films", *IEEE International Symposium on Micromechatronics and Human Science*, pp. 29-34.
- [3] Kloeck B., Collins S. D., de Rooij N. F., and Smith R. L. (1989) "Study of Electrochemical Etch-Stop for High-Precision Thickness Control of Silicon Membranes", *IEEE Trans. Electron Devices*, Vol. 36, No. 4, pp. 663-669.
- [4] Fricke J., and Obermeier E. (1993) "Cantilever beam accelerometer based on surface micromachining technology", *J. Micromech. Microeng.*, Vol. 3, pp. 190-192.
- [5] Plaza J. A., Esteve J., and Lora-Tamayo E. (1998) "Simple technology for bulk accelerometer based on bond and etch back silicon on insulator wafers", *Sensors and Actuators A*, Vol. 68, pp. 299-302.
- [6] Im S., and Atluri S.N. (1989) "Effect of a Piezo-Actuator on a Finitely Deformed Beam Subjected to General Loading", *AIAA Journal*, Vol.27, No.12, pp.1801-1807.
- [7] Ha S.K., Keilers C., and Chang F.K. (1992) "Finite Element Analysis of Composite Structures Containing Distributed Piezoceramic Sensors and Actuators", *AIAA Journal*, Vol.30, No.3, pp.772-780.
- [8] Gianchandani Y. B., and Crary S. B. (1998) "Parametric Modeling of a Microaccelerometer: Comparing I- and D-Optimal Design of Experiments for Finite-Element Analysis", *Journal of Microelectromechanical Systems*, Vol. 7, No. 2, pp. 274-282.
- [9] van Kampen R. P., and Wolfenbittel R. F. (1998) "Modeling the mechanical behavior of bulk-micromachined silicon accelerometers", *Sensors and Actuators A*, Vol. 64, pp. 137-150.
- [10] Nemirovsky Y., Nemirovsky A., Muralt P., and Setter N. (1996) "Design of a novel thin-film piezoelectric accelerometer", *Sensors and Actuators A*, Vol. 56, pp. 239-249.
- [11] Doebelin E. O. (1990), *Measurement Systems Application and Design*, McGraw-Hill, 4<sup>th</sup> ed.
- [12] Phadke M. S. (1989), *Quality Engineering Using Robust Design*, Practice-Hall, Inc., Englewood Cliffs, NJ, USA.
- [13] Sze S. M. (1994), *Semiconductor Sensors*, John Wiley & Sons, Inc.